served the same reactions with the enzyme from the procaryote *Streptomyces glaucescens*.

ACKNOWLEDGMENTS

We thank N. Bild and Dr. A. L. Lorenzi for acquisition of mass spectra.

REFERENCES

Barlin, G. B., & Perrin, D. D. (1966) *Q. Rev., Chem. Soc. 20*, 75–101.
Böttcher, G., & Kiese, M. (1960) *Naturwissenschaften 47*, 157.
Capdevielle, P., & Maumy, M. (1982) *Tetrahedron Lett. 23*, 1573–1576.
Capdevielle, P., & Maumy, M. (1987) *Actual. Chim. 4*, 5–11.
Clayson, D. B., & Garner, R. C. (1976) in *Chemical Carcinogens* (Searle, C. E., Ed.) ACS Monograph 173, pp 366–461, American Chemical Society, Washington, DC.
Entsch, B., Ballou, D. P., & Massey, V. (1976) *J. Biol. Chem. 251*, 2550–2563.
Fieser, L. F. (1930) *J. Am. Chem. Soc. 52*, 5204–5241.
Frederick, C. B., Mays, J. B., Ziegler, D. M., Guengerich, F. P., & Kadlubar, F. F. (1982) *Cancer Res. 42*, 2671–2677.
Grünanger, P. (1979) *Methoden Org. Chem. (Houben-Weil) 7(3b)*, 235–349.
Guillochon, D., Esclade, L., Cambou, D., & Thomas, D. (1984) *Ann. N.Y. Acad. Sci. 434*, 214–218.
Horner, L., & Sturm, K. (1955) *Chem. Ber. 88*, 329–338.
Job, D., & Dunford, H. B. (1976) *Eur. J. Biochem. 66*, 607–614.
Lerch, K. (1981) *Met. Ions Biol. Syst. 13*, 143–186.
Lerch, K. (1983) *Mol. Cell. Biochem. 52*, 125–138.
Lerch, K. (1987) *Methods Enzymol. 142*, 165–169.
Mason, H. S. (1957) *Adv. Enzymol. Relat. Areas Mol. Biol. 19*, 79–223.
Mason, H. S. (1965) *Annu. Rev. Biochem. 34*, 595–634.
Mason, H. S., Fowlks, W. B., & Peterson, E. W. (1955) *J. Am. Chem. Soc. 77*, 2914–2915.
McEven, W. K. (1936) *J. Am. Chem. Soc. 58*, 1124–1129.
Nigh, W. G. (1973) in *Oxidation in Organic Chemistry* (Trahanovsky, W. S., Ed.) pp 1–96, Academic, New York.
Ogawa, H., Nagamura, Y., & Ishiguro, I. (1983a) *Hoppe-Seyler's Z. Physiol. Chem. 364*, 1059–1066.
Ogawa, H., Nagamura, Y., & Ishiguro, I. (1983b) *Hoppe-Seyler's Z. Physiol. Chem. 364*, 1507–1518.
Prinz, W., & Savage, N. (1977) *Hoppe-Seyler's Z. Physiol. Chem. 358*, 1161–1163.
Radzik, D. M., Roston, D. A., & Kissinger, P. T. (1983) *Anal. Biochem. 131*, 458–464.
Schäfer, W. (1964) *Prog. Org. Chem. 6*, 135–163.
Schoot Uiterkamp, A. J., & Mason, H. S. (1973) *Proc. Natl. Acad. Sci. U.S.A. 70*, 993–996.
Suatoni, J. C., Snyder, R. E., & Clark, R. O. (1961) *Anal. Chem. 33*, 1894–1897.
Teuber, H. J., & Dietz, K. H. (1965) *Angew. Chem. 77*, 913.
Tomoda, A., Shirasawa, E., Nagao, S., Minami, M., & Yoneyama, Y. (1984) *Biochem. J. 222*, 755–760.
Wilcox, D. E., Porras, A. G., Hwang, Y. T., Lerch, K., Winkler, M. E., & Solomon, E. I. (1985) *J. Am. Chem. Soc. 107*, 4015–4027.

# Ribonuclease Structure and Catalysis: Effects of Crystalline Enzyme, Alcohol Cryosolvents, Low Temperatures, and Product Inhibition†

A. L. Fink,* D. Kar, and R. Kotin
*Division of Natural Sciences, University of California, Santa Cruz, California 95064*
*Received December 29, 1986; Revised Manuscript Received July 9, 1987*

ABSTRACT: In order to determine the necessary conditions to stabilize intermediates in ribonuclease A catalysis at subzero temperatures for structural studies, we have examined the suitability of alcohol-based cryosolvents. On the basis of thermal denaturation transition curves, the enzyme is in the native conformation in high concentrations of ethanol and methanol, provided the temperature is suitably low. The effects of methanol on the catalytic properties for the hydrolysis for mono- and dinucleotide substrates also are consistent with the absence of adverse effects of the cosolvent. Significant methanolysis occurs in the presence of methanol as cosolvent. The kinetics of 2′,3′-CMP hydrolysis are complicated by severe competitive product inhibition, both in aqueous and in methanolic solvents, accounting for the previously observed effect of substrate concentration on the observed $K_m$. Computer-aided analysis allowed the determination of the inhibition constant as a function of experimental parameters. The reaction of ribonuclease A with 2′,3′-CMP was investigated at subzero temperatures. The turnover reaction could be made negligible at temperatures below −60 °C at pH* 3–6 in 70% methanol and below −35 °C at pH* 2.1. The rate of the catalytic reaction with crystalline enzyme was compared to that of enzyme in solution for both 2′,3′-CMP and the dinucleotide CpC. The rates were 50- and 200-fold slower, respectively, in the crystal. These investigations allowed calculation of the necessary conditions for NMR and X-ray diffraction experiments on the trapped enzyme–substrate intermediate.

The general outline of the catalytic mechanism of ribonuclease has been known for some time (Richards & Wyckoff, 1971; Usher et al., 1972; Eckstein et al., 1972). The main aspects in the hydrolysis of a polynucleotide include a two-stage process, in which the first stage involves an intramolecular displacement by the 2′-OH group of ribose of the 5′-(hydroxymethyl) group of the adjacent nucleotide to give a cyclic 2′,3′-phosphate. The second stage involves the hydrolysis of

† This research was supported by grants from the National Institutes of Health and the National Science Foundation.
* Address correspondence to this author at the Department of Chemistry, University of California, Santa Cruz, CA 95064.

0006-2960/87/0426-8571$01.50/0 

the cyclic 2′,3′-phosphate to yield a terminal 3′-monophosphate ester. The displacement at the phosphorus has been shown to take place by an in-line mechanism.

There are, however, still some key features of the catalytic mechanism that have not yet been elucidated, due to the transitory nature of the enzyme–substrate complex. Cryoenzymology (Douzou, 1977; Fink, 1977; Fink & Cartwright, 1981) has been found to be a valuable means of stabilizing transient intermediates in enzyme catalysis. The present investigation has been undertaken with the following goals in mind: first, to find a suitable cryosolvent system for RNase A;[1] second, to find conditions of pH and low temperature where the turnover (catalytic) reaction can be effectively stopped and an enzyme–substrate intermediate accumulated; third, to determine the conditions necessary to prepare any such detected intermediate in the crystalline state so that its detailed structure can be determined by X-ray diffraction (Fink & Petsko, 1981). In the course of achieving these aims we encountered some unusual kinetic properties associated with the catalytic reaction of RNAse with 2′,3′-CMP, which we show stem from a combination of strong competitive product inhibition by 3′-CMP and from a second substrate and product binding site. We have previously shown that the suitability of a mixed aqueous–organic cryosolvent system can be ascertained by examining the effects of increasing concentrations of cosolvent on the catalytic and structural properties of the enzyme (Fink & Geeves, 1979; Fink, 1979). NMR can also be very useful in this regard, if the protein is sufficiently soluble in the cryosolvent for such a procedure. We have recently reported a detailed investigation into the stability of RNase A in aqueous methanol solvents (Fink & Painter, 1987).

## Experimental Procedures

*Materials.* Ribonuclease A was obtained from Calbiochem and Sigma. The enzyme was further purified by chromatography on Sephadex SPC-25, eluting with 0.13 M phosphate, pH 6.5, buffer. The RNase A fraction was then extensively washed free of phosphate by ultrafiltration with an Amicon PM-10 membrane and deionized, distilled water. 2′,3′-CMP and 3′-CMP were obtained from P-L Biochemicals. Reagent-grade buffer materials and solvents were used in the preparation of cryosolvents and buffers. Crystals of RNase A were grown from 60% ethanol, pH* 5.5 at 25 °C.

*Methods.* Cryosolvents were prepared on a v/v basis at 0 °C as described previously (Fink & Geeves, 1979). Steady-state and low-temperature kinetics were determined with a Cary 118 spectrophotometer equipped with a thermostated brass cell holder. Fluorescence measurements were performed with a Perkin-Elmer MPF-4 instrument. Neslab or Heto low-temperature, circulating, constant-temperature baths were used to maintain constant temperatures (±0.2 °C), with ethanol as coolant. Temperature measurements were made with Omega thermocouple probes. Values of pH*, the apparent protonic activity in the cryosolvent, were measured with a combination glass electrode at 0 or 25 °C and extrapolated to subzero temperatures (Hui Bon Hoa & Douzou, 1973). Enzyme and substrate solutions were mixed at subzero temperatures by methods previously described (Fink & Geeves, 1979).

[1] Abbreviations: RNase A, bovine pancreatic ribonuclease A; 2′,3′-CMP, cytidine 2′,3′-phosphate; 3′-CMP, cytidine 3′-phosphate; 5′-AMP, adenosine 5′-phosphate; CpC, cytidylyl(3′–5′)cytidine; NMR, nuclear magnetic resonance.

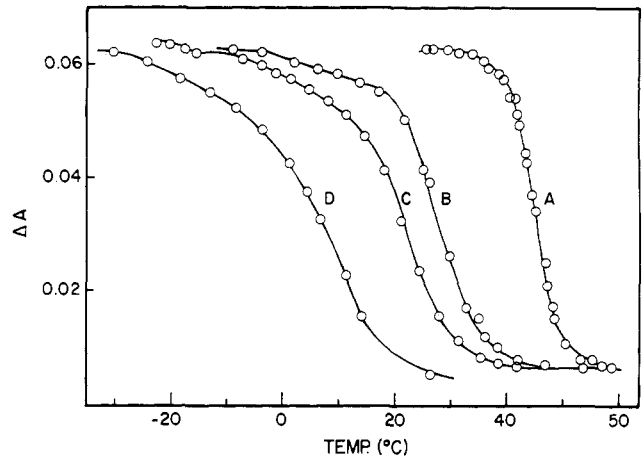


FIGURE 1: Thermal denaturation transition for RNase A in the presence of alcohols. The reaction was monitored at 286 nm. A = aqueous, B = 50% (v/v) methanol, C = 70% methanol, and D = 65% ethanol. Protein concentration was $2.9 \times 10^{-5}$ M, pH* 3.0 for A–C and pH* 2.8 for D. The curves were fully reversible.

Thermal denaturation transition curves were determined by changes in absorbance at 286 nm with 0.4 mg/mL solutions of RNase A. The reaction was fully reversible up to at least 70% methanol and 60% ethanol. The Arrhenius plots were calculated from initial velocity data for pH* 2.1 and 6.0 and from analysis of complete reaction curves for pH* 5.0 $^{31}$P NMR experiments were carried out on a Varian XL-100 instrument with a multinuclear (MONA) probe or a Jeol FX-100 instrument.

Kinetic analyses were performed with iterative curve-fitting procedures, in particular a program based on that of Bevington (1969), as modified by Morris et al. (1980) and subsequently adapted and expanded for use with a microcomputer system (Koerber & Fink, 1987). Data for complete reaction curves were used, with models for mono- and biexponential curves, Michaelis–Menten kinetics, and the Michaelis–Menten scheme with competitive product inhibition. Complete reaction curves were also analyzed graphically with the integrated form of the Michaelis–Menten equation for product inhibition (Cornish-Bowden, 1976).

## Results

Methanol-based cryosolvents are the ones of choice in cryoenzymological investigations because of their relatively low viscosities and low freezing points (Douzou et al., 1976), especially in cases where a flow cell will be used in X-ray diffraction experiments or for NMR experiments. Since RNase A crystals can be grown in aqueous ethanol, we initially investigated ethanol- and methanol-based cryosolvents for their effects on RNase A structure and catalysis.

*Effects of Cosolvent: Denaturation Transition.* The greater hydrophobicity of alcohols relative to water would be expected to result in thermodynamic destabilization of the protein's native state when in alcohol-based cryosolvent. In order to assess the magnitude of this effect, we have examined the thermal denaturation transition of RNase A in some aqueous ethanol and methanol solvent systems. As can be seen from Figure 1, the transition is indeed moved to lower temperatures in the presence of 50–70% alcohol, relative to the value in aqueous solution. It is interesting to note that the cooperativity of the transition is drastically reduced in the presence of the higher concentrations of alcohol. We attribute this to the presence of partially folded intermediate states, which are stabilized by the relatively hydrophobic cosolvent (Biringer & Fink, 1982; Fink & Painter, 1987). The data in Figure 1

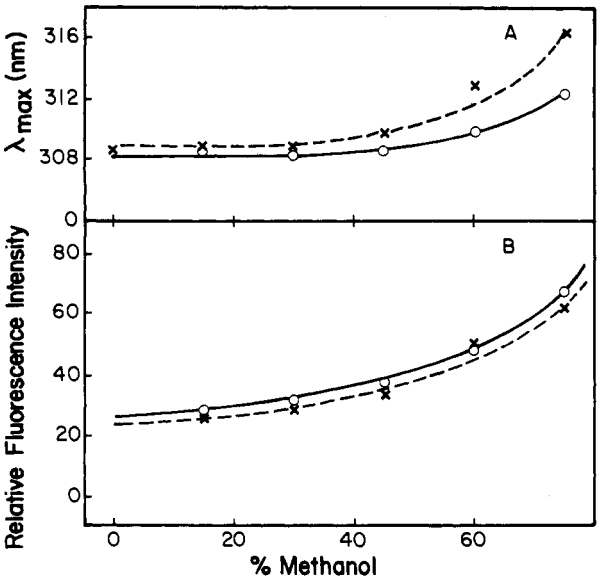


FIGURE 2: Effect of methanol on the fluorescence emission of RNase A (O) and *N*-acetyl-L-tyrosine ethyl ester (×): (A) emission maxima; (B) emission intensity at the maxima. pH* 5.0; −0.9 °C.

indicate that the native state predominates at subzero temperatures in these solvent systems.

*Intrinsic Spectral Probes.* The intrinsic spectral properties of the enzyme, e.g., fluorescence, provide a useful means of probing for cosolvent-induced structural effects. It is expected that spectral changes will occur due to solvent effects on exposed chromophoric groups and that these will manifest themselves as smooth monotonic changes in the signal as the cosolvent concentration changes. Perturbations of the protein structure, on the other hand, will result in sharp breaks in such plots (Fink, 1979). RNase has no tryptophan residues but six tyrosine residues, which will contribute to the near-UV spectral properties. Smooth monotonic changes in the fluorescence quantum yield and emission maximum are observed when the methanol concentration is increased from 0 to 70% at 0 °C (Figure 2). Similar effects are noted with the model compound *N*-acetyl-L-tyrosine ethyl ester, indicating that the majority of the fluorescence emission of RNase A comes from solvent-exposed Tyr residues. The circular dichroism spectrum of RNase A in 50% methanol, pH* 3 and 6, −20 °C (i.e., fully native enzyme), has also been found to be very similar to that in aqueous solution (B. Lustig and A. L. Fink, unpublished results).

*Cosolvent Effects on Catalytic Properties.* Measurement of the enzyme's catalytic parameters in the presence of cosolvent is a very sensitive means of detecting possible solvent effects. The stability of RNase A in 60% aqueous ethanol is revealed by the fact that the enzyme can be crystallized from this medium and the crystals then shown to be catalytically active in either the crystalline state or after subsequent dissolution into aqueous solution (see below). The stability of the enzyme in 70% methanol at 0 °C was determined by incubation at pH* 5.0. Assays of aliquots indicated a 6% decrease in catalytic activity toward 2′,3′-CMP over a 5-day period, a value within the experimental error.

We have previously shown the utility of determining the effects of increasing concentration of organic cosolvents on catalytic parameters such as $k_{cat}$, $K_m$, and $K_i$ (Fink, 1979). In Figure 3 are shown the effects of increasing methanol concentration on the values of $k_{cat}$, $K_m$, and $k_{cat}/K_m$ for the catalysis of 2′,3′-CMP at pH* 5.0, 0.5 °C, as determined from initial velocity experiments. A linear increase in $k_{cat}$ and a log-linear increase in $K_m$ are observed for increasing methanol

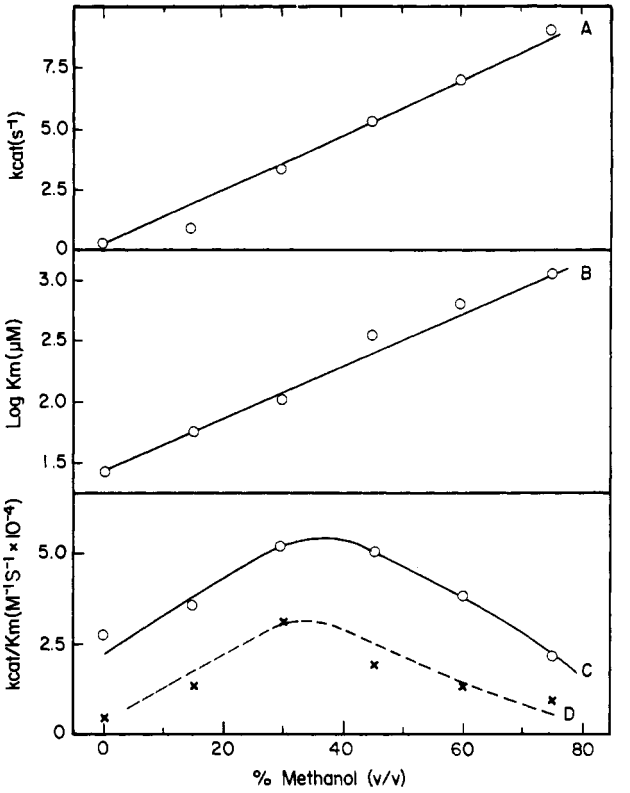


FIGURE 3: Effect of methanol on the catalytic parameters of the RNase A catalyzed hydrolysis of 2′,3′-CMP: (A) effect on $k_{cat}$; (B) effect on $K_m$; (C and D) effects on $k_{cat}/K_m$. Conditions: 0.5 °C, pH* 5.0, and 0.2 M acetate buffer. Panels A, B, and D were determined from initial velocities, with enzyme concentrations of the order of 0.05 mM (to minimize product inhibition effects); substrate concentrations were (0.1–10) × $K_m$. Panel C was obtained from complete reaction curves with $E_0$ = 0.5 μM and $S_0$ = 10–15 μM.

Scheme I

$$E + S \underset{}{\overset{K_s}{\rightleftharpoons}} ES \xrightarrow{k_2} I \begin{cases} \xrightarrow{k_3[H_2O]} E + P_1 \\ \xrightarrow{k_4[MeOH]} E + P_2 \end{cases}$$

concentration. It has been shown that methanol can act as a competing nucleotide with water in the RNase-catalyzed hydrolysis of this substrate (Findlay et al., 1962), resulting in the formation of cytidine 3′-phosphate methyl ester. The reaction scheme is thus as shown in Scheme I, where $P_1$ = 3′-CMP, $P_2$ = 3′-methyl ester of CMP, and $k_3$ and $k_4$ are the rate constants for hydrolysis and methanolysis, respectively. Under these experimental conditions, we calculate that the methanolysis rate is 170 times greater than that of hydrolysis.

Figure 3 also shows a plot of $k_{cat}/K_m$ vs percent methanol obtained from complete reaction curves. The data for 0 and 15% methanol come from analysis of the reaction curve assuming competitive product inhibition (see below), whereas at higher methanol concentrations the curves were monoexponential and were analyzed directly for the first-order rate constant. The data for 30% methanol were fit equally well by a first-order reaction or the Michaelis–Menten scheme for competitive product inhibition. These phenomena reflect the much weaker affinity of RNase A for the methyl ester of 3′-CMP, which becomes the major product at higher concentrations of methanol. Both the initial velocity data and that of the complete reaction curves rise to a maximum around 35% methanol.

The effect of pH* on the catalytic reaction was determined at −10 °C with 2′,3′-CMP as substrate and 60% ethanol as

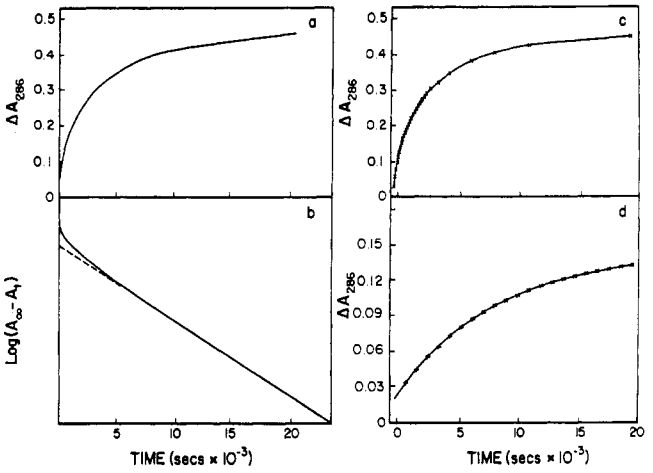


FIGURE 4: Biphasicity due to strong competitive product inhibition in the RNase A catalyzed hydrolysis of 2′,3′-CMP. (a–c) $E_0$ = 2.2 μM, $S_0$ = 500 μM, pH 5.0, 0.1 M acetate, and 1.5 °C. Panel a shows the complete reaction curve. Panel b shows a semilog plot to illustrate the biphasic nature of the data. Panel c shows the data (×) fitted to the integrated Michaelis–Menten equation with competitive product inhibition with $k_{cat}$ = 0.15 $s^{-1}$, $K_m$ = 45.2 μM, and $K_p$ = 11.8 μM. The data also fit a biexponential curve with $k_{obsd}$ = 1.35 × $10^{-3}$ and 1.9 × $10^{-4}$ $s^{-1}$, with amplitude ratios of 0.46:1. The data do not fit the simple integrated Michaelis–Menten equation, indicating that $K_m$(app) < $10S_0$. Panel d shows the effect of a high concentration of 3′-CMP on the reaction. The experimental data (×) have been fit to a single-exponential curve (solid line) with $k_{obsd}$ = 1.1 × $10^{-3}$ $s^{-1}$. Conditions for panel d were $E_0$ = 4 μM, $S_0$ = 150 μM, [3′-CMP] = 800 μM, pH 5.0, 25 °C, and 0.1 M acetate.

solvent. The pH–rate profile for $k_{cat}/K_m$ under these conditions resembles that reported in aqueous solution with the exception of a somewhat broader pH-optimum region. The calculated p$K$*'s are 4.6 and 6.8 which can be compared with the corresponding values in aqueous solution, at 25 °C, of 5.4 and 6.4 (del Rosario & Hammes, 1969). We should point out that the latter values were calculated with 0.1 M NaCl and 0.1 M acetate buffer, compared to an ionic strength of 0.05 M in the cryosolvent. It is well-known that the rates of RNase catalyses are very dependent on both ionic strength and specific salt ions. There will also be an effect due to the difference in temperature reflecting the heat of ionization of the imidazoles responsible for the p$K$'s. In the cryosolvent, $K_m$ showed a broad minimum (63.8 ± 6 μM) with p$K$*'s at 4.1 and 6.7; $K_p$ (for product inhibition) was essentially independent of pH* from 3.9 to 6.7 (31 ± 5 μM). The limiting value of $k_{cat}$ was 3.3 × $10^{-2}$ $s^{-1}$ under these conditions.

*Product Inhibition Effects.* Walker et al. (1975) have remarked upon the fact that the reported values of $K_m$ for the RNase-catalyzed hydrolysis of 2′,3′-CMP vary significantly with the substrate concentration range investigated. They attribute this to multiple binding sites for substrate and to two different, catalytically active, conformations of the enzyme. Dimers of ribonuclease A have been reported to give nonhyperbolic saturation curves for cyclic nucleoside monophosphate substrates (Piccoli & D'Alessio, 1984). Deviations from linearity in initial velocity curves have also been reported, especially at lower pH values (Herries et al., 1962). We noticed that complete reaction progress curves for the RNase A catalyzed hydrolysis of 2′,3′-CMP, under conditions of $[S]_0 \ll K_m$(app), which should have obeyed first-order kinetics, appeared biphasic (Figure 4). This phenomenon was noted in both aqueous and ethanol solvent systems, in the pH range 2–7. The reaction curves were fit very well by a model of two successive first-order reactions, with rate constants differing typically by a factor of 5 (but dependent on $E_0$ and $S_0$). The biphasicity was observed whether the reaction was monitored by changes in absorbance or with a pH-stat.

Table I: Effects of Varying Substrate and Product Concentration on $K_m$ and $K_p$ for the RNase A Catalyzed Hydrolysis of 2′,3′-CMP[a]

| [2′,3′-CMP] (μM) | [3′-CMP] (μM) | $K_m$ (μM) | $K_p$ (μM) | method of analysis |
|---|---|---|---|---|
| 50–1000 | 0 | 41.5 | 17.3 | *b* |
| 5–70 | 35, 62 | 40[f] | 8 | *c* |
| 30–310 | 0 | 32 | 16.6 | *d* |
| 60–312 | 400–500 | 42 | 2.8 | *e* |
| | | 3 | 7 | *d* |
| 150 | 400–800 | 40 | 2.6 | *e* |
| 500[g] | | 5.3 | 12.5 | *b* |
| 77[h] | 0 | 30.1 | 7.0 | *b* |

[a] Unless stated otherwise, the conditions were pH 5.0, 0.1 M acetate, and 25.0 °C. [b] Curve fitting to integrated Michaelis–Menten equation with competitive product inhibition. [c] Initial velocity. [d] Linearized form of the integrated Michaelis–Menten expression, after Cornish-Bowden (1976). $K_p$ obtained from replots of the intercepts. [e] From first-order analysis, assuming $V_{max}/K_m$(app) = $[V_{max}/K_m(lim)]$ $(1 + P/K_p)$. [f] Assumed value. [g] Conditions were pH 5.0, 0.1 M acetate, and 1.5 °C. [h] Conditions were pH 6.0, 0.1 M acetate, and 0.2 °C.

A number of possible sources of the biphasicity were investigated. These indicated that strong competitive product inhibition by 3′-CMP was the major factor responsible. The integrated Michaelis–Menten equation for a scheme involving competitive product inhibition is given by eq 1 (Cornish-Bowden, 1976), where $S_0$ represents initial substrate concentration and $K_p$ is the inhibition constant for product inhibition. Using a five-parameter iterative curve fitting program, it was possible to accurately analyze complete reaction curves to yield values of $V_{max}$, $K_m$, and $K_p$ (the other two parameters are $A_0$ and $A_\infty$). Some representative data are shown in Figure 4 and Table I. The integrated Michaelis–Menten equation can also be represented in a linear form (eq 1), in which $K_p$ for competitive product inhibition can be estimated from replots of the intercepts of reactions starting with different substrate concentrations. Values in good agreement with those obtained from curve-fitting were found with this analysis (Table I).

$$\frac{t}{\ln (S_0/S)} = \frac{1}{V}(1 - K_m/K_p)\frac{S_0 - S}{\ln (S_0/S)} + \frac{K_m}{V}(1 + S_0/K_p) \quad (1)$$

Confirmation that 3′-CMP was indeed responsible for the biphasicity in the reaction progress curves was obtained in experiments in which acid phosphatase was present. In this case conditions were chosen so that, as soon as 3′-CMP was produced by RNase catalysis, the acid phosphatase would hydrolyze the sugar–phosphate bond, thus destroying the 3′-CMP. In a typical experiment, with 0.93 mM 2′,3′-CMP, pH 5.0, and 0.1 M acetate ($E_0$ = 3.0 μM), the reaction curve was biphasic in the absence of acid phosphatase. On repeating the experiment with the addition of ≥0.1 mg/mL acid phosphatase, the biphasicity disappeared.

With complete reaction curves, starting with six different concentrations of 2′,3′-CMP, ranging from 50 to 1000 μM, the curve fitting analysis gave values of $k_{cat}$ = 3.3 ± 1.0 $s^{-1}$, $K_m$ = 41.5 ± 4.5 μM, and $K_p$ = 17.3 ± 0.8 μM, at pH 5.0, 25 °C, and 0.1 M acetate. A value of $K_m$ = 42 μM was obtained from replots of data analyzed graphically by means of eq 1 with data from five substrate concentrations ranging from 60 to 312 μM.

Experiments were carried out in the presence of various concentrations of 3′-CMP in order to "saturate" the enzyme with product, so as to remove the time-dependent variation in the 3′-CMP concentration. Three different procedures were

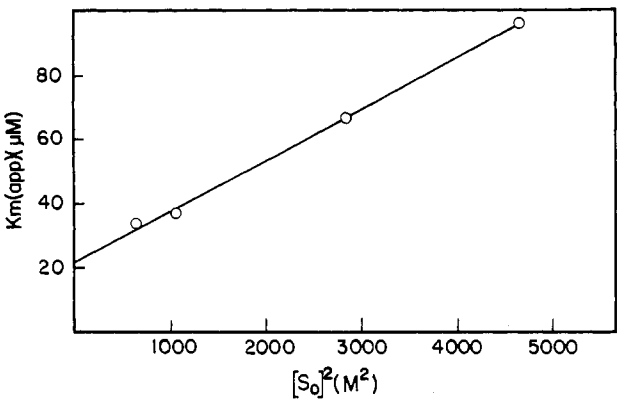


FIGURE 5: Effect of substrate concentration on $K_m$(app) in the presence of excess 3′-CMP. Conditions: [3′-CMP] = 460 μM, pH 5.0, and 25 °C. The data are plotted as $K_m$(app) vs $[S_0]^2$. The values of $K_m$(app) were obtained from the linearlized version of the integrated Michaelis–Menten equation.

used. In one case sufficiently large concentrations of 3′-CMP were used to make the reaction first order [$S_0 \ll K_m$(app)]. In this instance, for concentrations of 3′-CMP from 400 to 800 μM, a value of $K_p = 2.6 \pm 0.5$ μM was obtained (25 °C, pH 5.0, 0.1 M acetate) assuming $k_{obsd} = V_{max}/[K_m(1 + P/K_p)]$ (Figure 4d). Another approach was to measure initial velocities at low substrate and relatively low excess product concentrations. In this case a value of $K_p = 8 \pm 1$ μM was calculated for [3′-CMP] = 35 and 62 μM. The third method utilized replots of the linearized form of the integrated Michaelis–Menten equation for high concentrations of product. This gave a value of $K_p = 3$ μM for [3′-CMP] = 450 μM (Table I). From the variation in $K_p$ with concentration of 3′-CMP, it appears that the value of $K_p$ is probably significantly lower in the presence of high concentrations of 3′-CMP.

Even taking strong competitive product inhibition into consideration, the kinetics results of a variety of experiments suggested that more complex phenomena were involved. For example, not only is $K_p$ dependent on product concentration, but $K_m$ was found to be dependent on substrate concentration in the presence of excess 3′-CMP ($P_0 \gg S_0 \gg K_p$). As shown in Figure 5, a plot of $K_m$ vs $[S_0]^2$ was linear and empirically fit

$$K_m(\text{app}) = K_m(1 + S^2/K)$$

Extrapolation to $S_0 = 0$ gave a value of $K_m$(app) = 22 μM.

*Catalytic Reaction at Subzero Temperatures.* The goal of these experiments was to find conditions where turnover is negligible and an intermediate on the catalytic pathway can be accumulated and stabilized. For $^{31}$P NMR experiments it is necessary to use high enzyme concentrations. Given the limited solubility of RNase A at pH* ≥4, these experiments were carried out in the pH* range 2–3.

The catalytic reaction of ribonuclease with 2′,3′-CMP was monitored by changes in absorbance in the vicinity of 290 nm at a variety of temperatures in both aqueous ethanol and methanol solvent systems. In the temperature range of −10 to −30 °C, linear Arrhenius plots were observed. Some values calculated for the energies of activation for these reactions with 2′,3′-CMP as substrate are 12.4 ± 1.5 kcal mol$^{-1}$ for $k_{cat}/K_m$ for 50% methanol, pH* 2.1, and 13.2 ± 1.5 kcal mol$^{-1}$ for $k_{cat}/K_m$, with approximate values of 13.5 for $k_{cat}$, 3.1 for $K_p$, and 4.0 kcal mol$^{-1}$ for $K_m$ for 60% ethanol, pH* 6.0.

Some typical rate data for the reaction with 2′,3′-CMP at subzero temperatures are shown in Table II. At temperatures below −35 °C at pH* 2.0–2.4 or below −60 °C at the pH optimum (pH* ≥3), the turnover reaction was essentially

Table II: Ribonuclease Reactions with 2′,3′-CMP at Subzero Temperatures

| solvent[a] | pH* | temp (°C) | $E_0$ (μM) | $S_0$ (μM) | $k_{obsd}$ (μM)[b] | $V_i/E_0$ (s$^{-1}$) |
|---|---|---|---|---|---|---|
| 60% EtOH | 6.0 | −7.2 | 2.6 | 200 | | 3.1[c] |
| 60% EtOH | 6.0 | −13.7 | 2.6 | 200 | | 1.0[c] |
| 60% EtOH | 6.0 | −20.5 | 2.6 | 200 | | 0.8[c] |
| 60% EtOH | 6.0 | −29.9 | 2.6 | 200 | | 0.2[c] |
| 80% EtOH | 5.3 | −19.1 | 1.3 | 66 | $6.2 \times 10^{-3}$ | |
| 70% MeOH | 3.0 | 0.6 | 2.5 | 500 | | $3.0 \times 10^{-2}$ |
| 70% MeOH | 3.0 | −19.7 | 2.5 | 500 | $1.7 \times 10^{-3}$ | $1.8 \times 10^{-2}$ |
| 70% MeOH | 3.0 | −30.0 | 2.5 | 500 | $5.0 \times 10^{-4}$ | $7.2 \times 10^{-3}$ |
| 70% MeOH | 3.0 | −38.8 | 2.5 | 500 | | $2.1 \times 10^{-3}$ |
| 70% MeOH | 3.0 | −44.7 | 5 | 500 | | $3.3 \times 10^{-4}$ |
| 70% MeOH | 3.0 | −60.6 | 7.4 | 280 | [d] | |
| 70% MeOH | 3.8 | −22.0 | 27 | 200 | $1.0 \times 10^{-4}$ | |
| 70% MeOH | 4.9 | −22.0 | 27 | 195 | $1.3 \times 10^{-3}$ | |
| 70% MeOH | 5.3 | −24.1 | 29 | 110 | $5.2 \times 10^{-3}$ | |
| 70% MeOH | 3.7 | −61 | 5 | 140 | [d] | |
| 50% MeOH | 2.2 | −40.0 | 1700 | 4600 | [d] | |
| 50% MeOH | 2.5 | −35.0 | 61 | 4600 | $\leq 5 \times 10^{-5}$ | |

[a] MeOH = methanol, EtOH = ethanol. [b] Pseudo-first-order rate constant for the turnover reaction. [c] $k_{cat}$. [d] Negligible rate, i.e., turnover essentially absent.

negligible even with high enzyme concentrations. Attempts to measure $k_{cat}$ and $K_m$ as a function of temperature down to −60 °C were confounded by the limited solubility of the substrate and the increase in $K_m$ noted with decreasing temperatures. For example, in one set of experiments with $S_0$ = 0.5 mM, pH* 3.0, and 70% methanol, $K_m$ increased to 0.35 mM at −29.5 °C. The reaction was very slow at temperatures below −30 °C since the enzyme solubility considerably limits the enzyme concentration that can be used. With pseudo-first-order rate constants from these experiments, an energy of activation of about 9 kcal mol$^{-1}$ was calculated for the range 0 to −60 °C. A control experiment in which 3′-CMP (140 μM) was added in lieu of substrate at −59.2 °C showed no evidence of any time-dependent changes.

*Reactivity of Crystalline RNase A in Cryosolvents.* X-ray crystallography is the method of choice for determining the detailed structures of low-temperature-stabilized enzyme–substrate intermediates (Fink & Petsko, 1981). This procedure requires that the intermediate (or complex) be in the crystalline state. There are a number of prerequisites that must be satisfied before the actual X-ray diffraction experiment can be performed. These essentially involve ascertaining the appropriate conditions in which the crystalline intermediate can be formed and stabilized. The method chosen to accomplish this was as follows: crystals of RNase A would be grown in aqueous ethanol (Carlisle et al., 1974), they would be assayed for catalytic activity (in the crystalline state), and then the rate of crystalline enzyme-catalyzed substrate hydrolysis would be determined in cryosolvent at temperatures where turnover is relatively rapid. By comparison of the turnover rates of the enzyme in solution and crystalline states, a correction factor can be obtained that will allow estimation of the rate of intermediate formation and breakdown in the crystalline enzyme, given the known rates in the solution phase.

In a typical set of experiments, three RNase A crystals (grown in 30–40% ethanol) (approximately 0.6 × 0.3 × 0.2 mm) were transferred to 80% ethanol or 70% methanol, pH* 5.3. In order to be at a temperature below the thermal denaturation transition, it was desirable to work at temperatures of −20 °C or lower. The catalytic hydrolysis of 2′,3′-CMP was monitored at 284 nm. A slow increase in absorbance was observed. Aliquots of the supernatant were assayed during the reaction to measure the concentration of any dissolved enzyme. After completion of the reaction, the crystal was

Table III: Comparison of Activity of Crystalline and Dissolved Ribonuclease A

| state | $k_{obsd}$ ($s^{-1}$) | |
|---|---|---|
| | 2′,3′-CMP[a] | CpC[b] |
| crystalline | $1.6 \times 10^{-4}$ | $6.8 \times 10^{-4}$ |
| dissolved | $7.0 \times 10^{-3}$ | $1.4 \times 10^{-1}$ [c] |

[a] Conditions were 80% ethanol, pH* 5.4, −19 °C, $E_0$ = 30 μM, and $S_0$ = 310 μM. [b] Conditions were 70% methanol, pH* 5.5, −1.0 °C, $E_0$ = 3.8 μM, and $S_0$ = 180 μM. [c] The actual experiment was run with $E_0$ = 1.0 μM, and the rate constant was corrected for the different concentration in the experiment with crystalline enzyme.

dissolved in aqueous solution and assayed to determine the enzyme concentration. Control reactions were run with dissolved enzyme under otherwise identical conditions, so as to arrive at a comparative rate for the dissolved enzyme. The reaction rates were then normalized to the same enzyme concentration, and the ratio of crystalline to dissolved enzyme rates was determined (Table III). Similar experiments were carried out with the dinucleotide substrate CpC. For the cyclic phosphate substrate the reaction was 50-fold slower in the crystal. For the dinucleotide substrate the crystalline enzyme reaction was 200-fold slower than the dissolved enzyme reaction. Crystals were also shown to be active toward both 2′,3′-CMP and CpC under the following experimental conditions: 60% ethanol or 70% methanol, pH* 5.5, and 0 °C.

*$^{31}P$ NMR Experiments.* Preliminary experiments were carried out to determine whether a low-temperature-stabilized intermediate (presumably the trapped noncovalent enzyme–substrate complex) could be detected under conditions where the turnover reaction had been stopped due to a combination of low temperature and nonoptimal pH*. In a typical experiment at −35 °C, pH* 2.1–2.4, and 50% methanol, the reaction of 3 mM ribonuclease A with 15 mM 2′,3′-CMP was monitored for several hours. The only resonances observed were those of the substrate and the external standard trimethyl phosphite. No formation of product (3′-CMP) was observed. On warming the solution to 0 °C or above, the formation of product (3′-CMP) was observed. A preliminary experiment at −70 °C, 70% methanol, and pH* 2.7 revealed only exchange broadening of the substrate resonance and no evidence for any new species in the chemical shift region of substrate or product.

## Discussion

*Cosolvent Effects.* Clearly the effect of cosolvent on the catalytic properties of the enzyme will be the most sensitive and relevant measure of the potential suitability of a cryosolvent. In the present case the use of alcohols as cosolvents leads to possible complications in interpretation of the observed results due to the nucleophilicity of the cosolvent and consequent competition between hydrolysis and transesterification. This is reflected in the observed increase in $k_{cat}$ as a function of increasing methanol concentration (Figure 3). Previous studies (Findlay et al., 1962) have shown that the product of methanolysis is the expected methyl ester of 3′-CMP. The linearity of the $k_{cat}$ vs methanol concentration plot in Figure 3 implies neither a change in rate-determining step nor cosolvent-induced structural effects on the protein.

The log–linear relationship between $K_m$ and methanol concentration is expected. It is well documented (Maurel, 1978; Fink, 1979) that the relatively more hydrophobic cryosolvent leads to a hydrophobic partitioning effect on substrate binding; with the less polar cryosolvent the driving force for the substrate to seek the more nonpolar active site environment is decreased. Consequently, substrate binding becomes weaker and $K_m$ increases. Since the relationship between the solubility of the substrate and the hydrophobicity of the cryosolvent is a linear free energy one, a log–linear plot is expected. The data imply that hydrophobic interactions are important in the binding of 2′,3′-CMP to RNase A. The increase in $k_{cat}$ with increasing methanol concentration implies that the rate-limiting step is the breakdown of the intermediate I in Scheme I. As discussed in detail elsewhere (Coll & Fink, 1987), the expression for $K_m$ includes terms from the microscopic rate constants and is given by

$$K_m = \frac{(k_3[H_2O] + k_4[MeOH])K_s}{k_2 + k_3[H_2O] + k_4[MeOH]}$$

which reduces to

$$K_m = \frac{(k_3[H_2O] + k_4[MeOH])K_s}{k_2}$$

Consequently, there is an additional component to the increase in $K_m$ with increasing methanol concentration that comes from the term in the numerator and thus parallels the observed increase in $k_{cat}$.

The bell-shaped dependence of $k_{cat}/K_m$ vs percent methanol (Figure 3) reflects the opposing effects of methanol acting as a nucleophile to increase $k_{cat}$ (via methanolysis, Scheme I) and to decrease $K_m$ by increasing the solvent hydrophobicity. The values of $k_{cat}/K_m$ as determined from initial velocities differ from those determined by direct measurement of $k_{cat}$ and $K_m$ or their ratio (first-order conditions) due to the complications from strong competitive product inhibition, the initial velocity values being least reliable.

The pH–rate profile for the free enzyme is of the same shape in the cryosolvent as in aqueous solution but with somewhat different p$K$ values, as is to be expected from the effects of cosolvent and low temperature. At −10 °C, in 60% ethanol the value of p$K^*_1$ is 4.6 compared to 5.2 in aqueous solution, 25 °C, consistent with the cationic nature of the imidazole responsible for the ionization. Interestingly, the value of p$K^*_2$ appears unchanged by the presence of the cosolvent. However, this results from opposing effects of temperature and cosolvent on the p$K$ of the cationic group. A decrease in temperature of 35 °C will cause an increase of almost 1 pK unit.

One means of directly assessing the consequences of cosolvent on the enzyme's structure is to monitor the intrinsic spectral properties as a function of cosolvent concentration. Linear or smooth monotonic changes, as observed in Figure 2 for the effects on the fluorescence emission, are consistent with the lack of structural perturbations induced by the cosolvent. If such structural changes do occur, they are manifested as sharp breaks in such plots (Fink, 1979). Confirmation that high alcohol concentrations do not significantly affect the structure of RNase A in solution is found in the NMR spectra of the native state in aqueous methanol, which are very similar to those in aqueous solution (Biringer & Fink, 1982). Detailed analysis of the aromatic region of the proton NMR spectrum of RNase A in the presence of methanol, at temperatures at which the native state predominates, indicates a virtually identical structure with that in aqueous solution (Biringer, 1985). In addition, crystallographic results comparing the structures of crystalline ribonuclease S and A, grown in high salt, 2-methyl-2-propanol (40%) or ethanol (30–40%), show no differences in structure due to the solvent (Carlisle et al., 1974; Martin, 1976; Borkakoti et al., 1982; Wlodawer et al., 1982; Campbell & Petsko, 1987).

As can be expected, the thermodynamic destabilization of the system caused by the presence of the relatively hydrophobic cosolvent is manifested in part by decreased stability of the

native state (Figure 1). The low degree of cooperativity in these melting curves reflects the significant population of partially folded species during the unfolding transition (Biringer & Fink, 1982). A detailed report of the effects of methanol on the stability of ribonuclease A has been published recently (Fink & Painter, 1987). This study demonstrated that the general behavior of the protein e.g., the effects of pH or guanidine hydrochloride, was similar to that in aqueous solution. At temperatures below the beginning of the thermal unfolding transition (e.g., −15 °C for 70% methanol, pH* 3.0), the protein is native by such physical criteria as circular dichroism and NMR.

Considering all the evidence for cosolvent effects on the catalytic and structural properties of RNase A, we conclude that aqueous ethanol and methanol cryosolvents are quite satisfactory, provided the temperature is sufficiently low so that one is below the beginning of the thermal denaturation transition.

*Competitive Product Inhibition.* Although it has long been known that 3′-CMP binds tightly to RNase A and therefore acts as competitive product inhibitor, the extreme tightness of this binding, compared to that of the substrate and the ensuing consequences for the kinetics of the catalyzed hydrolysis of 2′,3′-CMP do not seem to have been generally recognized. Some of the earliest reported kinetic studies of the hydrolysis of 2′,3′-CMP reveal nonlinear initial velocities (Herries et al., 1962). An additional complication is that of the effect of ionic strength on the affinity of RNase A for 3′-CMP. For example, at $\mu$ = 0.01 M $K_p$ = 4 $\mu$M (Wigler, 1968), whereas at $\mu$ = 0.1 M ($KNO_3$) $K_p$ = 103 $\mu$M (Anderson et al., 1968) (pH 6.0, 25 °C). Reported values for $K_p$ at pH 5.0 are in the range of 100 ± 30 $\mu$M for 0.1 M ionic strength (Herries et al., 1962; Anderson et al., 1968). In fact, the enzyme's affinity for 3′-CMP is highly dependent on temperature, ionic strength, and specific ion effects (Anderson et al., 1968).

Walker et al. (1975) have pointed out that the reported values of $K_m$ for the RNase A catalyzed hydrolysis of 2′,3′-CMP range from $2.8 \times 10^{-4}$ to $7.2 \times 10^{-3}$ M, depending on the concentration range of substrate used. Although Walker et al. interpreted this observation differently, it is most simply, and adequately, explained by the competitive product inhibition effects. Our initial observation that the kinetics for the complete reaction curves of RNase A catalyzed hydrolysis of 2′,3′-CMP at 0 °C in aqueous and aqueous alcohol solvents, under conditions of $K_m(app) \gg S_0$, were biphasic rather than monophasic as expected was puzzling. However, computer simulations demonstrated that if competitive product binding occurred, with a value of $K_p \leq K_m$, then biphasic kinetics are to be expected.

Using either an iterative curve fitting procedure (for complete reaction curves) or the linearized form of the integrated Michaelis–Menten equation with product inhibition (for several values of $S_0$) permitted us to obtain values of the product dissociation constant. As indicated in Table I, good agreement is obtained between the two methods. The results show that the product binds considerably tighter than the substrate, assuming that $K_m$ reflects the substrate dissociation constant. If product inhibition is not taken into consideration, the observed values of $K_m$ from initial velocity experiments are found to be dependent on the substrate concentration chosen.

Experiments carried out in the presence of high concentrations of product revealed that the value for $K_p$ decreases by an order of magnitude (Table I). This suggests the possibility of a second site of interaction for 3′-CMP at high concentrations, which affects the binding in the active site. Support for such an interpretation is found in the observation that $K_m$ varies with substrate concentration in the presence of high concentrations of 3′-CMP (Figure 5).

One likely explanation of the substrate effect on $K_m$ is the following. Since the "normal" substrate for RNase is a polynucleotide and since maximum specificity is observed with dinucleotides, there must be at least two nucleotide binding sites. Both the substrate 2′,3′-CMP and the product 3′-CMP could potentially bind in either site. For expository purposes we will call the site in which the substrate (2′,3′-CMP) binds and is hydrolyzed the catalytic site; the other will be referred to as the "secondary" site. Competitive product inhibition occurs when 3′-CMP binds in the catalytic site. It is possible that binding of a nucleotide in the secondary site causes small structural changes in the enzyme which result in tighter binding of ligands in the catalytic site. Support for this notion comes from the report of Simons (1971), which indicates that binding of 3′-CMP induces a conformational change in the enzyme. A second binding site for 3′-CMP at high concentrations has been reported by Hammes and Walz (1969) and for 5′-AMP by Myer and Schellman (1962). Richards and Wyckoff (1971) report that both nucleotide binding sites (B1 and B2 in their parlance) can be simultaneously occupied by 3′-CMP and that at high pyrimidine concentrations the so-called B2′ alternative site can be occupied. Evidence has also been presented that purines can bind to the so-called purine binding site, which corresponds to the site we have called the secondary site, and can induce a conformational change (Arus et al., 1982). Binding of 2′,3′-CMP or 3′-CMP in the secondary site when they are present at high concentrations is the most likely explanation of the observed effects of substrate concentration on $K_m$ and product concentration on $K_p$. This is also the probable explanation of the effect of adenosine in increasing the rate of hydrolysis of 2′,3′-CMP (Wieker & Witzel, 1967), which has also been attributed to a second conformation of the enzyme (Rubsamen et al., 1974).

*Reactivity of the Crystalline Enzyme.* The pioneering studies of Doscher and Richards (1963) established that crystals of ribonuclease S and amorphous RNase A are catalytically active toward cyclic 2′,3′-phosphates of pyrimidine nucleotides. There are basically two approaches that can be taken to form a crystalline intermediate stabilized at subzero temperatures. These are either to diffuse the substrate into preexisting crystals of the enzyme under appropriate low-temperature conditions or to form the intermediate in solution and allow it to crystallize at suitably low temperature. In the present case the latter approach is precluded by the relatively rapid breakdown of the intermediate compared to the anticipated rate of crystallization.

Our results indicate that crystals (of a size suitable for X-ray diffraction experiments) of RNase A in aqueous ethanol or methanol at subzero temperatures are catalytically active, although significantly less so then the dissolved enzyme. The 4-fold greater rate reduction observed for the hydrolysis of CpC with the crystalline enzyme compared to that for 2′,3′-CMP presumably reflects the greater diffusional constraints on the larger dinucleotide substrate. We noted that crystals of ribonuclease A kept in 80% ethanol at pH* 3 at 0 °C, where the enzyme is substantially denatured in solution (Figure 1), became coated with an impermeable layer of denatured protein after a period of time. Cutting the enzymes up into smaller fragments revealed that it was only the surface layer that was inactive.

Since experiments with the dissolved enzyme indicated that the turnover rate was very slow at −70 °C, pH* 3.0, it was possible to estimate the necessary experimental conditions for the X-ray diffraction experiment as follows. We have previously shown (Fink, 1976) that the rate of intermediate transformation under essentially nonturnover conditions will be inversely proportional to the substrate dissociation constant ($K_I$ or $K_s$). Since the rate reduction observed with the crystalline enzyme is assumed to stem from diffusional constraints imposed by the crystal lattice (Fink & Petsko, 1981), the observed rate reduction in the turnover reaction can be attributed to this same factor. Thus knowing the rate of formation and breakdown of the intermediate in solution, one can estimate what the rates will be in the crystal. Since X-ray data collection for a high-resolution structure of RNase would take a week, one can estimate that if one wishes to lose no more than 2% of the intermediate per day that −70 °C (at pH* 5) would be a satisfactory temperature for the X-ray experiment. An additional safety factor exists in that if the substrate is present during the data collection period, a pseudo-steady-state system would be established, with the majority of the enzyme in the form of the intermediate (presumably the ES complex). Our results therefore provide the experimental information necessary for a crystallographic investigation of the structure of the low-temperature-stabilized enzyme–substrate complex. In a subsequent publication (Campbell & Petsko, 1987) the detailed crystallographic structure of the complex of the enzyme with 2′,3′-CMP, trapped at −70 °C, will be reported.

*Preliminary $^{31}P$ NMR Results.* The results of the low-temperature kinetic and X-ray experiments indicate that the ES complex between RNase A and 2′,3′-CMP can be trapped at suitably low temperature and pH*. The $^{31}P$ NMR experiments at −35 °C show no evidence of a detectable intermediate in the $^{31}P$ NMR spectra. We estimate that under the experimental conditions a minimum of 15% of the enzyme would have to be in the form of the intermediate to be observed, assuming that line broadening of the protein-bound phosphorus was not too severe. Since $K_m$ increases at low pH*, it is likely that the amount of bound substrate may have been quite low in these experiments. This is borne out by spectrophotometric observations that show no evidence of an intermediate, even though turnover did not occur, under comparable experimental conditions (−30 °C, pH* 2.1). It is also conceivable that there is no difference in the chemical shift of the phosphorus between the free and bound substrate states, but this seems unlikely. The most probable explanation as to why no intermediate was observed in the −70 °C experiment is that of line-broadening effects.

*Conclusions.* We have shown that aqueous ethanol or aqueous methanol cryosolvents have no adverse effects on the structural or catalytic properties of RNase A and are therefore suitable for mechanistic studies of the enzyme at subzero temperatures. Interesting kinetics phenomena occur with the cyclic phosphate substrate 2′,3′-CMP due to very tight product binding at low ionic strength, as found under cryoenzymological conditions. Experiments in 70% methanol have shown that the turnover reaction with 2′,3′-CMP can be made negligible, and the experimental conditions necessary to accumulate and stabilize the accumulated intermediate in the crystalline state have been determined, as a prerequisite to crystallographic structural studies of the intermediate.

## ACKNOWLEDGMENTS

We are grateful for the help of Prof. T. James and Chris Serdahl with the $^{31}P$ NMR experiments. Some of the kinetics experiments were performed by Rob Wilson, an NSF undergraduate research participation (URP) student.

## REFERENCES

Anderson, D. G., Hammes, G. G., & Walz, F. G. (1968) *Biochemistry 7*, 1637–1645.

Bevington, P. R. (1969) *Data Reduction and Error Analysis for the Physical Sciences*, pp 232–242, McGraw-Hill, New York.

Biringer, R. G. (1985) Ph.D. Thesis, University of California, Santa Cruz.

Biringer, R. G., & Fink, A. L. (1982) *J. Mol. Biol. 160*, 87–116.

Borkakoti, N., Moss, D. S., & Palmer, R. A. (1982) *Acta Crystallogr., Sect. B: Struct. Crystallogr. Cryst. Chem. B38*, 2210–2217.

Campbell, R. L., & Petsko, G. A. (1987) *Biochemistry* (following paper in this issue).

Carlisle, C. H., Palmer, R. A., Mazumdar, S. K., Gorinsky, B. A., & Yeates, G. G. R. (1974) *J. Mol. Biol. 85*, 1–18.

Coll, R., & Fink, A. L. (1987) *Cryobiology 24*, 332–344.

Cornish-Bowden, A. (1976) *Principles of Enzyme Kinetics*, pp 144–146, Butterworths, London.

del Rosario, E. J., & Hammes, G. G. (1970) *J. Am. Chem. Soc. 92*, 1750–1758.

Doscher, M., & Richards, F. M. (1963) *J. Biol. Chem. 238*, 2399–2407.

Douzou, P. (1977) *Cryobiochemistry: An Introduction*, Academic, London.

Douzou, P., Hui Bon Hoa, G., Maurel, P., & Travers, F. (1976) *Handbook of Biochemistry and Molecular Biology*, 3rd ed. (Fasman, G., Ed.) Vol. 1, p 520, CRC Press, Cleveland, OH.

Eckstein, F., Saenger, W., & Suck, D. (1972) *Biochem. Biophys. Res. Commun. 46*, 964–971.

Findlay, D., Mathias, A. P., & Rabin, B. R. (1962) *Biochem. J. 85*, 134–139.

Fink, A. L. (1976) *J. Theor. Biol. 61*, 419–445.

Fink, A. L. (1977) *Acc. Chem. Res. 10*, 233–239.

Fink, A. L. (1979) *Adv. Chem. Ser. No. 180*, 35–54.

Fink, A. L., & Geeves, M. A. (1979) *Methods Enzymol. 63A*, 336–371.

Fink, A. L., & Cartwright, S. J. (1981) *CRC Crit. Rev. Biochem. 11*, 145–207.

Fink, A. L., & Petsko, G. A. (1981) *Adv. Enzymol. Relat. Areas Mol. Biol. 52*, 177–246.

Fink, A. L., & Painter, B. (1987) *Biochemistry 26*, 1665–1671.

Hammes, G. G., & Walz, F. G., Jr. (1969) *J. Am. Chem. Soc. 91*, 7179–7186.

Herries, D. G., Mathias, A. P., & Rabin, B. R. (1962) *Biochem. J. 85*, 127–134.

Hui Bon Hoa, G., & Douzou, P. (1973) *J. Biol. Chem. 248*, 4649–4656.

Koerber, D. G., & Fink, A. L. (1987) *Anal. Biochem. 165*, 75–87.

Martin, P. D. (1976) Ph.D. Thesis, Wayne State University.

Maurel, P. (1978) *J. Biol. Chem. 253*, 1677–1683.

Morris, R. G., Saliman, G., & Dunn, M. F. (1980) *Biochemistry 19*, 725–732.

Myer, Y. P., & Schellman, J. A. (1962) *Biochim. Biophys. Acta 55*, 361–368.

Piccoli, R., & D'Alessio, G. (1984) *J. Biol. Chem. 259*, 693–695.

Richards, F. M., & Wyckoff, H. W. (1971) *Enzymes (3rd Ed.) 4*, 647–806.

Simons, E. R. (1971) *Biochim. Biophys. Acta 251*, 126–131.

Usher, D. A. (1969) *Proc. Natl. Acad. Sci. U.S.A. 69*, 115–118.
Walker, E. J., Ralston, G. B., & Darvey, I. G. (1975) *Biochem. J. 147*, 425–433.
Wieker, H. J., & Witzel, H. (1967) *Eur. J. Biochem. 1*, 251–257.
Wlodawer, A., Bott, R., & Sjolin, L. (1982) *J. Biol. Chem. 257*, 1325–1332.

# Ribonuclease Structure and Catalysis: Crystal Structure of Sulfate-Free Native Ribonuclease A at 1.5-Å Resolution†

Robert L. Campbell and Gregory A. Petsko*
*Department of Chemistry, Massachusetts Institute of Technology, Cambridge, Massachusetts 02139*
*Received December 29, 1986; Revised Manuscript Received February 25, 1987*

ABSTRACT: The structure of native bovine pancreatic ribonuclease A, without the inhibitory sulfate anion normally bound at the active site, has been determined by X-ray diffraction at 1.53-Å resolution. Treatment of a crystal of ribonuclease containing sulfate with an alkaline buffer released most of the sulfate anions. On return to active pH, few of the side chains moved, and the backbone structure remained unchanged. The active site conformation was essentially unchanged except for the replacement of the sulfate anion by a water molecule, which is hydrogen-bonded to histidine-12 and to another water, and for a small movement of the side chain of lysine-41. Histidines-12 and -119, the catalytic basic and acidic residues, have not moved. Thus the distance between them, and the presence of an intervening water, prohibits the possibility of their being hydrogen-bonded together. The structure has been refined by restrained least squares to an *R* factor of 0.17. Analysis of individual atomic temperature factors indicates that the molecule has become less rigid in general but that some regions were particularly affected by loss of the sulfate, while others were relatively unaffected. The active site geometry of native ribonuclease A supports the original in-line mechanism of Rabin and co-workers and is in disagreement with the adjacent mechanism of Witzel and co-workers.

Bovine pancreatic ribonuclease A (RNase A) is a historical landmark in the study of protein structure and function. Because it has long been available in relatively large amounts in good purity, it has provided a model system to study the mechanisms of enzyme catalysis. RNase A was the first enzyme to be sequenced (Smyth et al., 1963; Potts et al., 1962) and one of the first for which X-ray diffraction revealed a three-dimensional structure (Kartha et al., 1967). A considerable amount of work has been done to study the crystal structures of both RNase A and the subtilisin-cleaved form, RNase S (Carlisle et al., 1974; Wlodawer et al., 1982; Wyckoff et al., 1967, 1970), and complexes of these with various inhibitors and substrate analogues (Richards et al., 1971; Richards & Wyckoff, 1973; Borkakoti, 1983). This is the second in a series of nine papers describing a combined low-temperature kinetics and crystallographic study of the structural basis for the catalytic power of RNase A.

Ribonuclease A, a monomeric enzyme of $M_r$ 13 683, is roughly kidney shaped with the active site located in a deep cleft. Figure 1 shows a stereoview of the α-carbon backbone of the native enzyme. The dot in the cleft shows the position of a bound sulfate ion (see below). The enzyme catalyzes the cleavage of RNA, leaving a nucleoside 3′-monophosphate, and is specific for pyrimidines on the 3′-side of the cleavage site.

In addition to the crystallographic work on RNase, many other physical and chemical experiments have been done to elucidate the mechanism of catalysis. The active site residues involved in catalysis have been examined by chemical modification. Two histidines and one lysine were found to be essential to enzymic activity. Carboxymethylation with iodoacetic acid modifies either histidine-12 or histidine-119, but not both, resulting in an inactivated enzyme (Crestfield et al., 1963). The enzyme can also be inactivated by dinitrophenylation of lysine-41 (Hirs et al., 1965). The activity versus pH curve is bell shaped, implicating a base of $pK_a = 5.22$ and an acid of $pK_a = 6.78$ in the free enzyme (Findlay et al., 1962). From kinetic and pH titration data a mechanism was proposed by Findlay et al. (1962) in which two histidines act as base and acid catalysts, while one lysine serves to position the phosphate group of the substrate. This was later elaborated upon by Roberts et al. (1969), who considered NMR and X-ray diffraction data as well as the earlier chemical modification and kinetic data and proposed that the two histidines were His-12 and His-119 and that the lysine was Lys-41.

In this in-line mechanism (Figure 2a), the histidines are on opposite sides of the phosphate moiety with His-12 acting as a base on the 2′-OH of the substrate and His-119 acting as an acid to protonate the 5′-oxygen of the leaving group in the first half of the reaction. The histidines reverse roles in the second half of the reaction: His-12 reprotonates the 2′-oxygen and His-119 deprotonates a water molecule which, again in an in-line manner, attacks the cyclic phosphate intermediate formed as the product of step 1. Lysine-41 appears to be in a position to stabilize the pentacoordinate transition states by either hydrogen-bonding or charge–charge interaction.

A different, adjacent mechanism (Figure 2b) was proposed by Witzel and co-workers (Witzel, 1963; Ruterjans & Witzel, 1969; Rubsamen et al., 1974) on the basis of structure–activity relationships of model substrates and NMR and kinetic ex-

† This work was supported by a grant from the National Institutes of Health (GM 26788).

0006-2960/87/0426-8579$01.50/0 